$Ag_2Cu_3Cr_2O_8(OH)_4$:

A new bidimensional silver-copper mixed - oxyhydroxide with in-plane ferromagnetic coupling

Nieves Casañ-Pastor*[‡], Jordi Rius[‡], Oriol Vallcorba[ǀ], Inma Peral[ǀ], Judith Oró-Solé[‡], Daniel S. Cook[#], Richard I. Walton[#], Alberto García[‡],David Muñoz-Rojas*[‡]

Supplementary material

Table of contents

1. Details of the structure refinement and coordinate tables

Indexing was successfully carried out by introducing 22 extracted peaks in TREOR90. The true solution (a=5.40, b=5.56, c=10.63 Å, α=80.55, β=69.50, γ=58.23°, V=255 Å³) had the best FOM [M(20)=10; F(20)=57 (0.0127, 28)]. The model-free profile refinement with Dajust,[1] using Mythen-II data, confirmed the unit cell: a= 5.3895(5), b= 5.5564(4), c= 10.6204(7)Å, α= 80.717(8), β= 69.485(6), γ= 58.370(7)°, R_{wp}= 0.035; χ^2= 1.44. The corresponding reduced unit cell at the end of the Rietveld refinement is a= 5.3329(1), b= 5.3871(1), c= 10.0735(1) Å, α= 80.476(1), β= 87.020(1), γ= 62.383(1)°, V= 252.8 Å³.

The crystal structure was solved by applying cluster-based Patterson-function direct methods in $P\overline{1}$ (Xlens_PD6[2]). The number of reflections was 253 for a resolution limit fixed at d_{min}=1.28 Å, which represented 63 refined phases. Default number of phase-refinement trials was 50. The Fourier map of the trial with best FOM showed most atoms of the Cu and Ag layers. For the initial Rietveld refinement, the expected mean cation-O distances were introduced as restraints. The irregularity of the coordination polyhedra of Cu^{2+} (Jahn-Teller effect) and Ag^+ (possible trend to linearity) posed some difficulties. However, the two longer Cu-O bonds in each octahedron could be established. The atomic coordinates of this model were further refined by density-functional theory (DFT) first-principles calculations (with no symmetry constraints), leading to 2.11, 2.11, 2.11, 2.44, 2.44, 1.68, 1.68 Å mean bond distances for the respective Cu(1), Cu(2), Cu(2'), Ag(1), Ag(1') , Cr(1)and Cr(1') coordination polyhedra. This set of coordinates was selected for the calculation of the individual expected bond lengths in the last restrained Rietveld refinement. The DFT results also confirmed the long Jahn-Teller Cu-O bonds already found by X-ray diffraction. The last Rietveld refinement with the DFT bond lengths introduced as restraints produced no significant residual increase [R_{wp}=0.088, χ=1.51].

References

(1)   Vallcorba, O.; Rius, J.; Frontera, C.; Peral, I.; Miravitlles, C. DAJUST: A Suite of Computer Programs for Pattern Matching, Space-Group Determination and Intensity Extraction from Powder Diffraction Data. *J. Appl. Crystallogr.* **2012**, *45*, 844–848.
(2)   Rius, J. Patterson-Function Direct Methods for Structure Determination of Organic Compounds from Powder Diffraction Data. *Acta Crystallogr. Sect. A* **2011**, *67*, 63–67.

Table S1: Final atomic coordinates of $Ag_2Cu_3Cr_2O_8(OH)_4$ refined from synchrotron powder X-ray diffraction data.

Atom	multiplicity	x/a	y/b	z/c
Cu1	1	0	0	0
Cu2	2	0.3355(5)	0.3341(6)	-0.0050(3)
Ag1	2	-0.3348(4)	0.1613(4)	0.5010(2)
Cr1	2	-0.0142(6)	0.5740(6)	0.2991(3)
O1	2	-0.0086(12)	0.6130(12)	0.1238(4)
O2	2	0.0012(15)	0.8457(14)	0.3515(8)
O3	2	0.2828(13)	0.2717(12)	0.3472(8)
O4	2	-0.3005(13)	0.5522(15)	0.3554(8)
OH1	2	0.3102(12)	-0.0020(13)	0.1032(7)
OH2	2	-0.3236(12)	0.2970(12)	0.0969(7)

a= 5.3329(1), b= 5.3871(1), c= 10.0735(1) Å, α=80.476(1), β=87.020(1), γ=62.383(1)°, V=252.8 Å^3, s.g. P-1. Full occupancies for all atoms. Refined isotropic displacement parameters U are 0.013(2) for Cu1, 0.013(2) for Cu2, 0.030(3) for Ag1, 0.020(2) for Cr1 and 0.026(2) Å^2 for the O atoms.

Table S2. Final Rietveld refined distances and DFT distance values (average value due to the presence of the symmetry center).

A1	A2	Ref. dist. (Å)	DFT dist. (Å)
Cu1	O1	2.26(1)	2.23
Cu1	OH1	2.00(1)	2.03
Cu1	OH2	2.07(1)	2.09
Cu2	O1	2.27(2)	2.22
Cu2	OH1	2.01(2)	2.02
Cu2	OH2	2.05(2)	2.09
Cu2	O1	2.05(2)	2.09
Cu2	OH1	2.24(2)	2.24
Cu2	OH2	2.02(2)	2.03
Ag1	O2	2.47(2)	2.47
Ag1	O3	2.41(2)	2.42
Ag1	O4	2.43(2)	2.43
Ag1	O2	2.36(2)	2.40
Ag1	O3	2.47(2)	2.45
Ag1	O4	2.43(2)	2.48
Cr1	O1	1.74(2)	1.72
Cr1	O2	1.67(2)	1.68
Cr1	O3	1.68(2)	1.67
Cr1	O4	1.66(2)	1.67

Table S3: : Positions of the atoms as determined by DFT calculations in which the structure was relaxed (no symmetry center was imposed). Atom numbering corresponds to Table S1. Atoms marked with ' denote partner atoms formally related by the symmetry center. The number sequence for hydrogen atoms corresponds to the matching oxygen atoms represented as OH(n).

| Atom	x/a	y/b	z/c
CU1	0.0000	0.0000	0.0000
CU2	0.3280	0.3388	0.9932
CU2'	0.6722	0.6635	0.9931
AG1	0.6620	0.1561	0.4947
AG1'	0.3316	0.8194	0.4959
CR1	0.9849	0.5587	0.2926
CR1'	0.0093	0.4127	0.6978
O1	0.9947	0.6176	0.1197
O2	0.9878	0.8295	0.3502
O3	0.2694	0.2508	0.3465
O4	0.6903	0.5338	0.3371
O1'	0.0044	0.3787	0.8705
O2'	0.0038	0.1286	0.6530
O3'	0.7247	0.7129	0.6377
O4'	0.3033	0.4289	0.6456
OH1	0.3248	0.9887	0.1001
H1	0.2999	0.0081	0.1966
OH2	0.6766	0.3042	0.0956
H2	0.6771	0.3026	0.1941
OH1'	0.6805	0.0149	0.8923
H1'	0.7187	0.0111	0.7954
OH2'	0.3166	0.7046	0.8959
H2'	0.3000	0.7368	0.7967

2. XPS survey spectrum
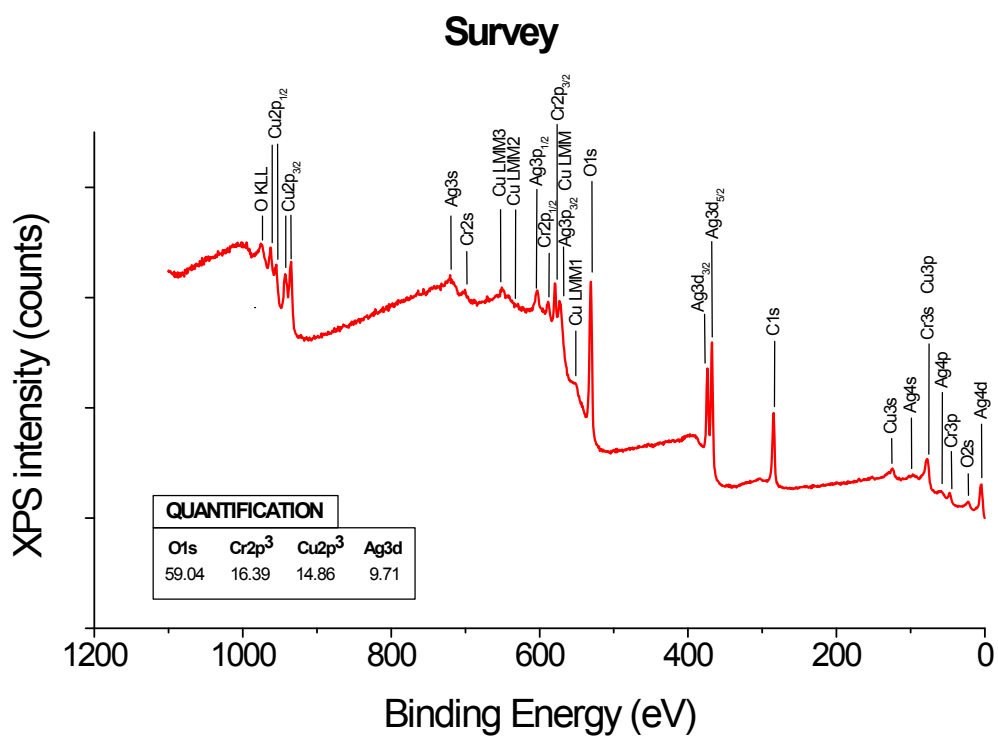
Survey

Figure S1: XPS survey spectrum with all peaks labeled: No other elements are present.
Quantification refers to atomic %

3. Susceptibility graphs
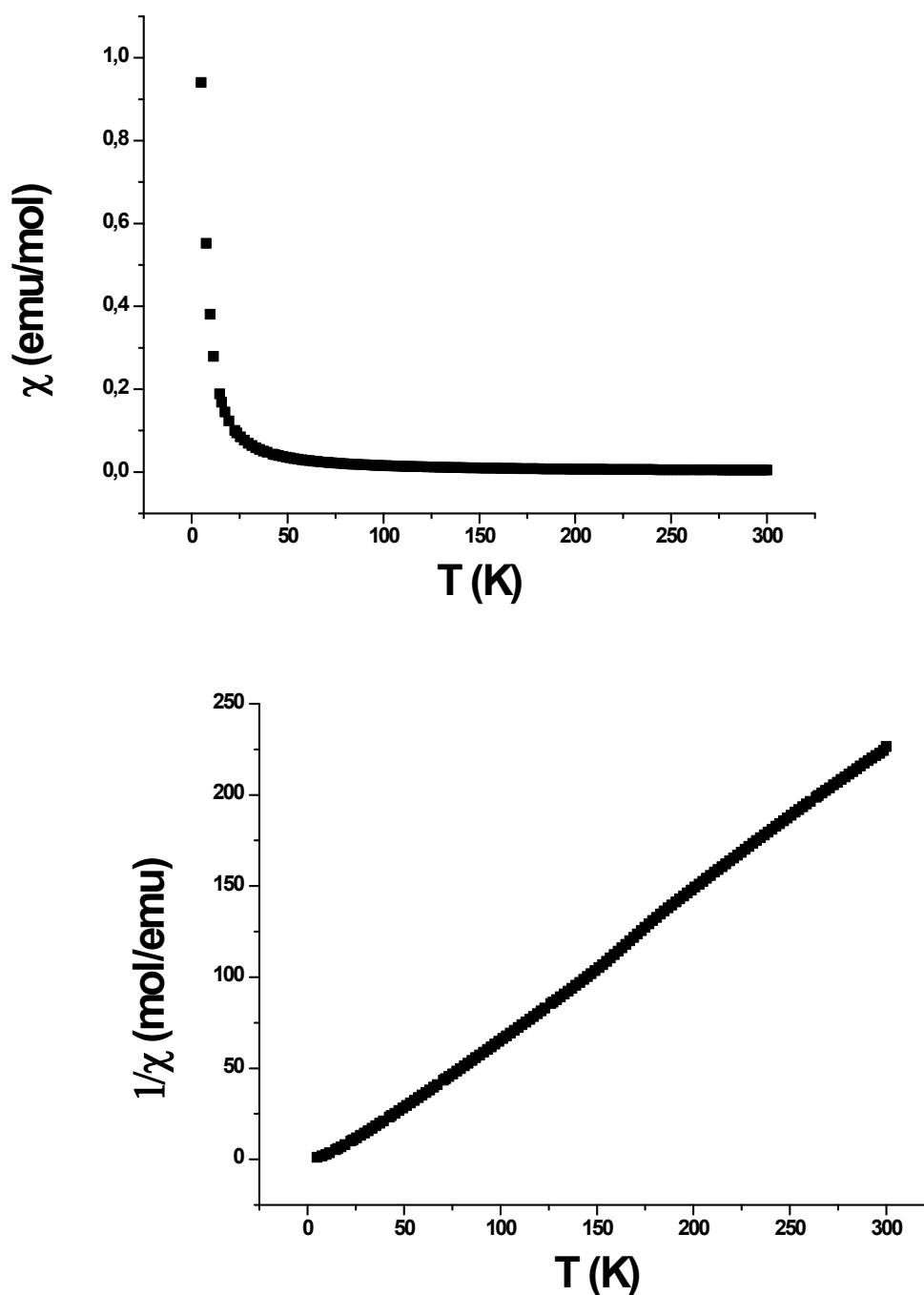

Figure S2. Top: Molar susceptibility vs. T. Bottom: Inverse of the Molar susceptibility vs. T (Data fitting evidences, below 200K, a lower 1/Chi value and a steeper rise of Chi than expected from Curie´s law, consistent with the presence of ferromagnetic coupling. The behavior of the effective moment shown in Fig. 6 in the main manuscript is a more transparent exhibition of this phenomenon). Molar data obtained from M, mass measured and formula weight, refers to 3 Cu.
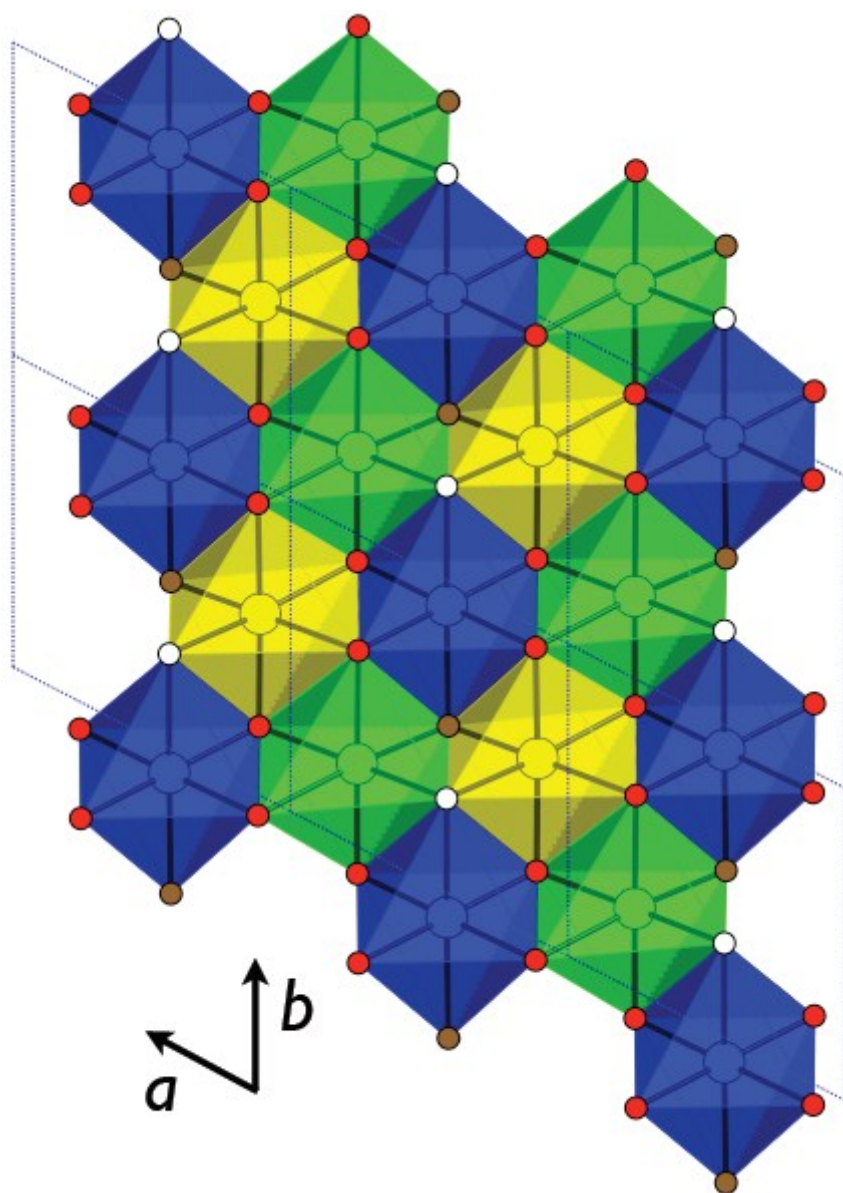
Figure S3. Detail of the pattern of edge-sharing octahedra in the brucitic layer. Oxygen atoms belonging to OH groups are depicted in red, and those associated to chromate groups are colored in white.
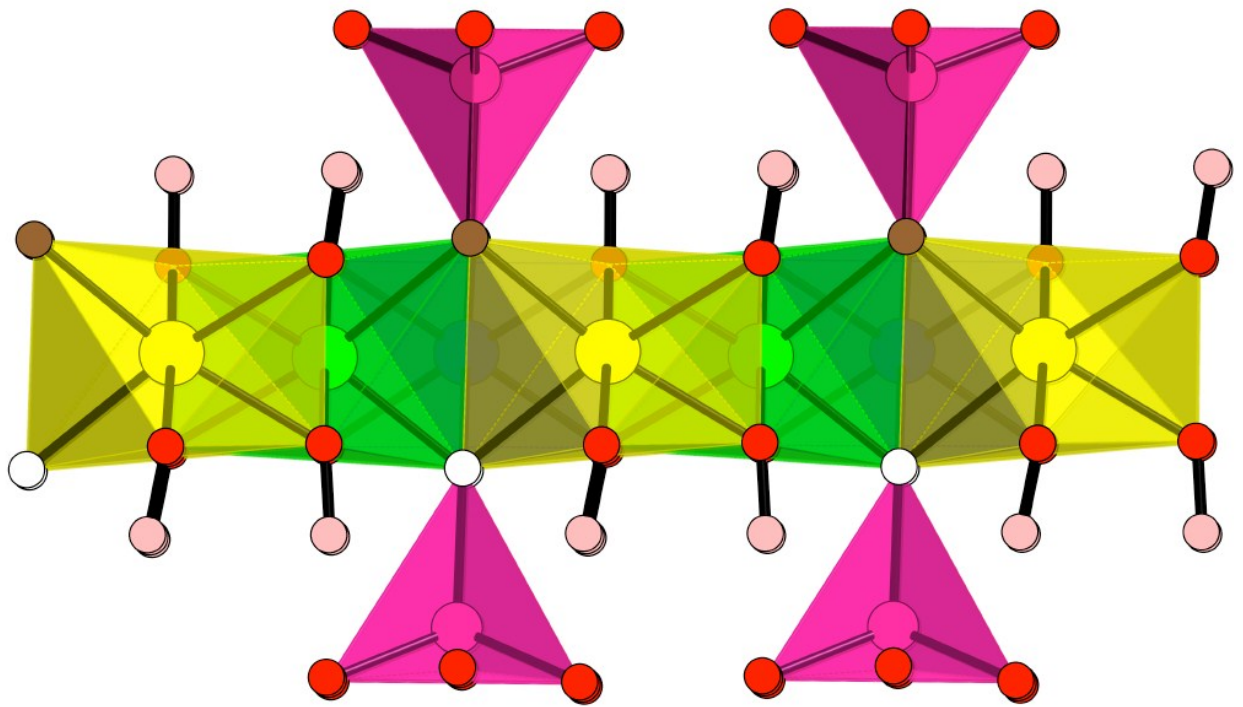
Figure S4. Side view of the Cu brucitic layer showing octahedral connections to neighboring Cr groups and OH elements.

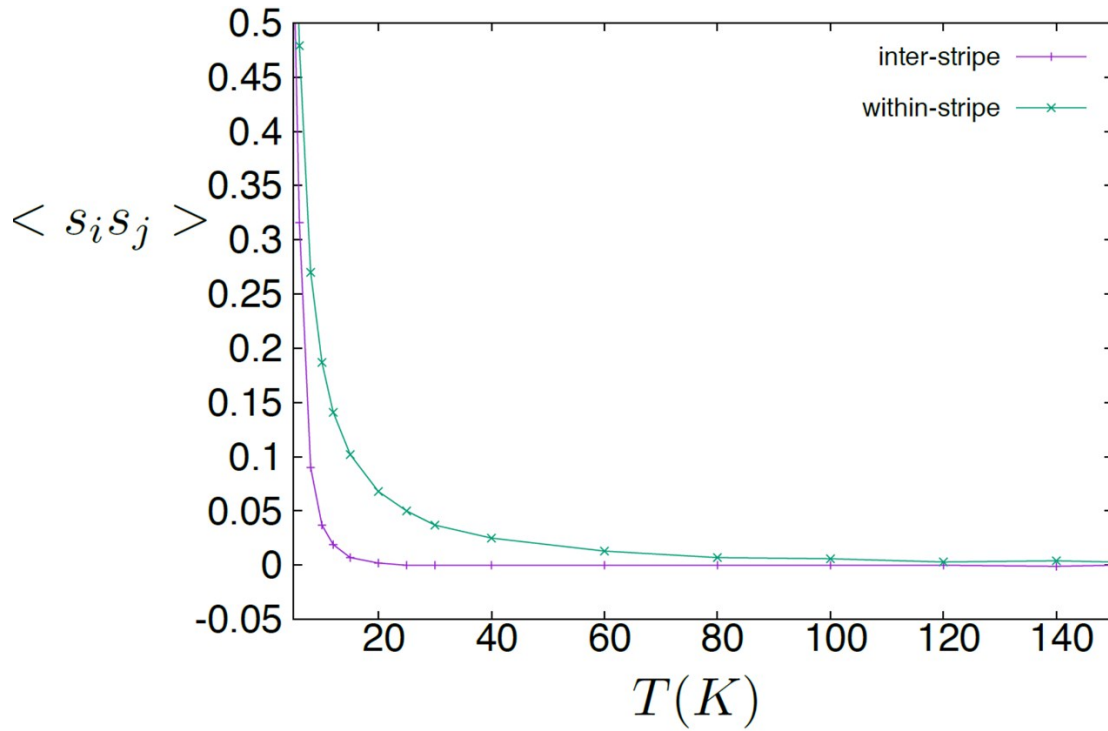## 3. Intra- and inter-stripe correlation graphs

Figure S5. Spin correlations as a function of temperature for sites on neighboring cells along the **a** cell vector (in neighboring stripes) and along the **b** cell vector (within a stripe). The intra-stripe correlations are evident already at high temperatures, but would only reach unity at very low temperature, which means that the stripes are not completely ordered in the experimental range.